Comparison of Different Detector Sensitivity Models for Transit Photometry and their Effects on Exoplanet Analysis

Kevin Sohn (260782138), Emma Klemets (260775167), and Lambert Francis (260861226)
Department of Physics, McGill University

This paper features the transit lightcurve analysis of three different exoplanets: CoRoT-2b, KELT-9b, and WASP-18b, all detected by the Spitzer Space Telescope. We examined how the use of different detector sensitivity models affected the planetary parameters of CoRoT-2b by performing MCMC on transit data. The sensitivity models used in this paper are the polynomial-type models, Fourier decomposition-type models, and a Gaussian Process model. The Gaussian Process model resulted in the best overall fit for both the raw transit lightcurve and the true astrophysical signal (white noise filtered), attributing three orders of magnitude more of the raw data as white noise than all other models. However, the runtime of the Gaussian Process model was just as great compared to the other models, requiring vastly more computing power. The Fourier models disagreed with both the Gaussian Process model and polynomial models on the value of CoRoT-2b's lightcurve offset ($\approx 10\sigma$ difference). This indicates that the choice of which detector sensitivity model to use can affect the outcome of the fit parameters significantly. We recommend utilizing multiple sensitivity models for exoplanet transit analysis to catch outliers. In this paper, we also discuss the planetary wind directions of CoRoT-2b, KELT-9b, and WASP-18b. We found that they all appear to blow westward based-on the negative lightcurve offset values.

I. INTRODUCTION

Space: the final frontier. Decades from now, the possibility of finding alien life will be just over the horizon. To detect life, we must be able to learn about the planets that may harbour life in excruciating detail. This is not a trivial task, but with the aid of recent advancements in exoplanet detection and analysis methods, we are one step closer to achieving this dream.

Unlike the vast majority of astrophysical sources in the universe, exoplanets do not generate their own light. It is not to say that exoplanets do not emit any light; they reflect light from their host stars, which is faint but detectable. However, the reflected starlight often gets obscured or overwhelmed by much stronger electromagnetic sources such as stars and galaxies. This makes directly observing exoplanets difficult because telescopes require the source photons to reach their detectors in order to resolve an image. A solution around this is to come up with clever indirect methods of exoplanet detection.

Over the decades, many indirect detection methods have been put forth and put to use by various research groups. One of the most successful exoplanet detection method is called Transit Photometry (TP), and is currently the most widely utilized method [1]. The concept behind TP is simple: it is a widely accepted fact that planets orbit around stars (not accounting rogue planets). From this fact, we can infer that the brightness of a star under observation will occasionally drop from its standard rate whenever a planet transits in front of said star (primary transit), where "in front" refers to the relative positions of the planet and the star with respect to the observer. By studying the properties of these periodic brightness dips, we can deduce properties about the transiting exoplanet.

As insinuated above, a secondary dip in brightness is also observed when studying exoplanet transits. These

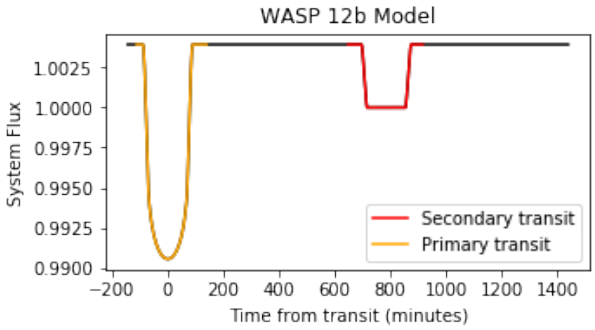

FIG. 1: Showcasing the idealized primary transit dip (orange) and secondary transit dip (red), without the planet's phasecurve.

are caused by the absence of planet reflected starlight as the planet transits behind its host star, which normally contributes to the baseline brightness of the planet-star system. Fig. 1 shows what an idealized primary and secondary transit curves look like. As you can see, the primary transit dip is much larger in magnitude than the secondary transit dip. This is not surprising considering that the planet blocks a good portion of starlight during primary transit compared to secondary transit, where the planet does not block any starlight.

A feature to note from Fig. 1 is how the primary transit dip curves towards the bottom whereas the secondary transit dip stays flat during the whole transit. This is due to an effect called limb-darkening, shown in Fig. 2, where the star appears redder and dimmer near its edges [2].

A surprising amount of information can be extracted from transit dips: the depth of the primary transit dip can accurately tell us about the star-to-planet radius ratio. Since the magnitude of this dip is only proportional to the size of the planet relative to the size of its host

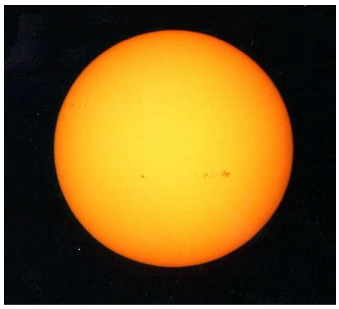

FIG. 2: An example of limb-darkening that is apparent when observing stars. [3]

star, the equation

$$\frac{\Delta f}{f} = \frac{R_p}{R_s} \tag{1}$$

allows for the calculation of the planet's radius, where f is the magnitude of the star's flux (observed brightness), Δf is the magnitude of the transit dip, R_s is the radius of the host star, and R_p is the radius of the planet.

The secondary transit can give information about the eccentricity of the orbit, as well as the star-to-planet luminosity ratio. The latter can be easily obtained by comparing the luminosity of the star during secondary transit (where the luminosity of the star is isolated) and during non-transit (where the luminosity of the star is coupled with the planet).

The advantage of using TP is its ability to accurately constrain the size of exoplanets [1]. However, no detection method is perfect, and TP is not without its downsides: Firstly, only the upper bound of an exoplanet's mass can be obtained using this method. Another detection method called the Radial Velocity Method must be used in conjunction with TP to obtain the actual mass of the planet [1]. Secondly, due to most exoplanets being much smaller than their host stars, there is a lower limit to the size of exoplanets we can detect. This is especially true for TP because if the planet is small enough, the transit dip may be obscured by the detector noise. This causes a bias towards planets around the size of Jupiter [4]. Lastly, extending the previous point, most exoplanets detected with TP are tidally-locked, meaning that the planet's year is equal to its day. This is because large planets in close proximity to their stars are most likely to tidally-lock [5]. This means that tidally-locked planets block out more starlight during transits and have shorter orbital periods than other types of planets. The combination of these two factors lead to pronounced transits dips with fast re-occurrence, making it easy for TP to detect [4].

As a side note on tidally-locked, or synchronous rotation, planets, there is a large temperature difference between the side of the planet that is constantly illuminated by the host star (dayside), and the side that is left unilluminated (nightside). From thermodynamics, we know that systems achieve thermal equilibrium if no barrier is present to prevent this from occurring. Then, the presence of such a extreme temperature gradient lead to winds forming in the planet's atmosphere in effort to achieve equilibrium.

Although most of the downsides for TP can be mitigated by complementing it with another detection method, noise is always a difficult nuisance to decrease. Fortunately, systematic noise, such as noise due to detector sensitivity, can be accounted for during data analysis.

Detector sensitivity is an issue with roots in fabrication; all pixels used to detect photons are not made equal. Moreover, these pixels are the most sensitive to light near their center, tapering off noticeably as one gets closer to the edge. For a space telescope such as Spitzer (the telescope that took our data), this is a big deal because the intra-pixel variations in sensitivity in tandem with the telescope free-floating in space (no anchors for stabilization) cause non-trivial systematic noise within the data [6].

One method is to come up with a detector sensitivity model to filter out the white noise and find the true astrophysical signal. One can achieve this by using a combination of Bayesian inference and Markov Chain Monte Carlo (MCMC) to find the best fit parameters for a model that discern true astrophysical signals from white noise. In literature, there is currently hot debate amongst exoplanet researchers on whose detector sensitivity model is the best.

In this paper, we study the transit lightcurves of three exoplanets detected by Spitzer: CoRoT-2b, KELT-9b, and WASP-18b. All three planets are tidally-locked. Therefore, by inspecting their dayside and nightside temperatures, in addition to offset, we can compare the magnitude and direction of the resulting winds. Furthermore, we compare the strengths and weaknesses of seven different detector sensitivity models to quell the debate once and for all; four models from literature and three models of our own creation, using CoRoT-2b data as a standard.

II. METHODS

The python package *starry* was used to initialize the planet-star system and to compute the ideal (without noise) lightcurve of the system for a set of given initial parameters. The proofs of these functions can be found in the *starry* documentation.

The planet-star system was initialized with 13 parameters: R_p, a, i, ϵ, $long_{peri}$, T_{orb}, T_{rot}, $t_{transit}$, q_1, q_2, L, $K_{1,1}$, and $K_{1,0}$. R_p denotes the radius of the planet in stellar radii; a is the orbital semi-major axis in stellar radii; i is the orbital inclination in degrees, ϵ is the eccentricity of the orbit; $long_{peri}$ is the longitude of pericenter in degrees; $Torb$, T_{rot}, and $t_{transit}$ are the orbital period, rotation period, and time of transit all in days; q_1 and q_2 are the first and second order terms of the quadratically limb-darked star model, respectively; L is the power ratio

between the planet and star. $K_{1,1}$ and $K_{1,0}$ represent the coefficient of the l=1, m=1 and l=1, m=0 spherical harmonic representing the exoplanets surface temperature distribution, respectively.

The sensitivity of the pixels were accounted for by multiplying the lightcurve returned by *starry* with a sensitivity model function. This means that our model for the data's lightcurve was of the form $system.lightcurve \times sensitivity\_function$.

Of the parameters in the *starry* system model, six were included as parameters to fit in the MCMC: R_p, q_1, q_2, L, $K_{1,1}$, and $K_{1,0}$. One additional parameter, σ, was included to account for the white noise in the data. The parameters of the sensitivity function were fit for in the MCMC and so added n parameters to the fit, if n is the number of parameters of the sensitivity function. This means that our MCMC fit for $n + 7$ parameters.

The MCMCs themselves were performed using the ensemble sampler software package *emcee*. The MCMC consisted of 50 to 80 walkers and a burn-in stage of 3000 to 5000 iterations, followed by another 2000 iterations to determine the parameters. An exception was made for the Gaussian Process sensitivity model (see section II A 3), which used 50 walkers and a burn-in stage of 700 iterations followed by another 700 iterations. Furthermore, only the second value of every data point was used for the MCMC instead of the full dataset. The reasoning was that the GP model is very computationally expensive compared to the other sensitivity models in this project, especially for a student laptop to handle.

The Parameters and their errors were extracted from the MCMC chain by assuming they were Gaussian distributed and calculating the median and standard deviation of each parameter's sample. These values were then used to calculate the offset of the lightcurve peak from the phase of the secondary transit (in degrees), using the equation

$$\text{offset} = arctan2(K_{1,1}, K_{1,0}) \times \frac{180}{\pi}. \tag{2}$$

Assuming that stars and planets emit as black bodies, we can also calculate the dayside and nightside temperatures from flux using the inverted Planck's Law,

$$T = \frac{hc}{k_B \lambda}(log(\frac{(1 + e^{(hc)/(k_B \lambda T_{star})} - 1)}{(fp_f star/R_p^2)}))^{-1}, \tag{3}$$

where T_{star} is the stellar effective temperature and $fp_f star$ is $L \cdot$ (planet flux(Ψ)) with Ψ being the angle from the center of the dayside hemisphere.

The uncertainties in offset and temperature were calculated with Monte Carlo simulations using Eq. II and Eq. II, where the size of the samples for each variable was 100,000.

A. Model Selection

Functions used to model detector sensitivity included polynomials of varying degrees, a Fourier decomposition, and a Gaussian Process (GP) model. The first two were chosen because the intra-pixel sensitivity variance is generally smooth, lending it to be modeled well by polynomial and trigonometric functions. However, modeling white noise of the data using a functional form imposes inherent bias; it uses preexisting theories to nudge the data into a specified form. The GP model avoids this by not having a fixed functional form, therefore not imposing any bias and being purely data driven.

1. Polynomial

Polynomial detector sensitivity models get their name from, as suggested, polynomials. These are possibly the most basic type of sensitivity models and they perform quite well for being so simple in construction. The idea behind them is to use polynomials of varying degree to model the smooth tapering of intra-pixel sensitivity. By controlling where the max/min of these polynomials occur, one can mimic the sensitivity of the pixels to a good approximation. We employ three polynomial type models: Quadratic, Cubic, and Quartic. It should be mentioned that these models are two dimensional polynomials to account for the motion of the star, which takes place in a plane in the pixel frame.

2. Fourier Decomposition

Fourier decomposition models are of our own creation and the idea is to model the intra-pixel sensitivity in a more general way than the polynomial models. Recall that a Fourier series is expressed in the form

$$f(t) = \frac{a_0}{2} + \sum_{n=1}^{\infty}[a_n \cos(\omega_n t) + b_n \sin(\omega_n t)], \tag{4}$$

where n is an integer ranging from one to infinity, $\omega_n = \frac{2\pi n}{T}$ is the angular frequency of varying n's, T is the period of the sinusoid, and a_n and b_n are the coefficients for cosine and sine, respectively.

We used three Fourier type models: n=2, n=3, and cosine. As the names suggest, the n=2 model uses two sine and cosine pairs and the n=3 model uses three sine and cosine pairs. The cosine model only consist of cosine terms in order to bias the model to find symmetric solutions. Symmetric as we want to model the pixel sensitivity tapering off symmetrically from the center of the pixel to its edges.

Model	R_p [Stellar radii]	L [Stellar luminosity]	$K_{1,1}$	$K_{1,0}$	σ [Normalized flux]	Offset [deg]	Dayside temp. [K]	Nightside temp. [K]
Quadratic	0.1600(7)	$2.97(9) \times 10^{-3}$	$-0.29(2)$	0.50(1)	$1.30(4) \times 10^{-6}$	$-30(2)$	1940(30)	1130(10)
Cubic	0.1608(7)	$2.96(9) \times 10^{-3}$	$-0.34(2)$	0.46(1)	$1.17(3) \times 10^{-6}$	$-36(2)$	1830(30)	1250(10)
Quartic	0.1608(6)	$3.0(1) \times 10^{-3}$	$-0.38(2)$	0.43(2)	$1.15(3) \times 10^{-6}$	$-40(2)$	1890(30)	1200(20)
Fourier n=2	0.1597(9)	$2.79(9) \times 10^{-3}$	$-0.03(3)$	0.574(3)	$2.56(7) \times 10^{-6}$	$-3(3)$	1920(30)	1040(10)
Fourier n=3	0.1589(9)	$2.73(9) \times 10^{-3}$	0.03(3)	0.574(3)	$2.40(6) \times 10^{-6}$	3(3)	1910(30)	1030(10)
Fourier cosine	0.157(1)	$3.1(1) \times 10^{-3}$	$-0.27(2)$	0.50(1)	$3.24(9) \times 10^{-6}$	$-28(2)$	2010(40)	1170(20)
Gaussian Process	0.162(1)	$3.1(4) \times 10^{-3}$	$-0.4(1)$	0.43(6)	$1.49(5) \times 10^{-3}$	$-40(10)$	1900(100)	1210(50)

TABLE I: MCMC fitted parameter for each detector sensitivity model are shown for the CoRoT-2b dataset. Description of the above parameters can be found in the methods section.

3. Gaussian Process

The idea of a Gaussian process is not to restrict the sensitivity model to a particular functional form. Instead, we have a probability distribution over different functions to avoid the bias of having a chosen function. The prior of the Gaussian process can also be adjusted to prefer smoother functions, which is desirable given the sensitivity is assumed to vary smoothly.

III. RESULTS & DISCUSSION

A. Model Comparison

To compare between different detector sensitivity models, we ran all of the models through just one exoplanet transit dataset. We picked planet CoRoT-2b for its relatively clean lightcurve and small data volume compared to KELT-9b and WASP-18b. Fig. 3 shows multiple instances of CoRoT-2b's lightcurve; three polynomial models, three Fourier decomposition models, and a GP model.

Qualitatively, notice how increasing the degree of the polynomial models does not drastically alter the shape of the resulting lightcurves. In comparison, the Fourier models have quite noticeable differences when it comes to the white noise properties of the blue curves (noisier) and the overall fit of the orange curves. We believe the reason for polynomial models having minor differences is due to polynomials adding linearly, whereas the Fourier models have more noticeable differences due to sines and cosines adding non-linearly; adding a higher order term to a polynomial cause less drastic deviations in value than adding an entire sine and cosine (especially since sine and cosine are orthogonal functions). Moreover, the right orange curve of the Fourier cosine model resembles the orange curve of the quadratic polynomial model more-so than the other Fourier models. This resemblance may be by construction because the intention of keeping only cosine terms in the Fourier series was to impose symmetric solutions to the detector sensitivity model, and quadratic polynomials are symmetric.

Although the polynomial and the Fourier models give good fits to the transit lightcurve, the GP model takes the cake for having the cleanest fits for both the left and right plots. The true astrophysical signal (right plot) for the GP model has the white noise filtered out greatly, which consequently results in the raw lightcurve (left plot) being noisier than the other two models. This is a good characteristic to see because it is indicative of a more discerning model. Overall, the GP model seems to give the best fits, with the polynomial model and the Fourier model being close second and third, respectively.

However, before making any conclusions, we must examine the sensitivity models quantitatively. Looking at Table I, we observe that the radius of the planet (R_p) and the dayside temperature is consistent within 2σ across all detector sensitivity models. Interestingly, the same cannot be said for the nightside temperatures. All parameters of the Fourier cosine model is within 2σ of the the quadratic model parameters (except white noise (σ)), exemplifying the similarity between the two models, quantitatively.

The Fourier n=2 and Fourier n=3 model parameters do not agree with all other models ($> 4\sigma$), including the Fourier cosine model. This trend is continued for planet luminosity (L), surface temperature distribution ($K_{1,0}$ & $K_{1,1}$), and offset. What all of the Fourier models do have in common is the fact that the white noise parameter (σ) is noticeably greater than the polynomial models, attributing at least twice as much of the raw data to white noise. Although that could be an advantageous property, there is a trade-off, because it is quite evident from the Fig. 3 that the Fourier models seemingly fit the raw data less appropriately. On the other hand, this is not an issue for the GP model because its white noise parameter is three orders of magnitude greater than all other models whilst fitting the raw data appropriately.

A big consequence of the Fourier n=2 and Fourier n=3 models having such large dissimilarities in offset but having minor dissimilarities in dayside and nightside temperatures is how that affects the interpretation of planetary winds. If one were to only use the Fourier n=2 and Fourier n=3 models in their exoplanet transit analysis, one might conclude that the planetary winds for CoRoT-2b are stronger/weaker and in the opposite direction than what one might conclude for the rest of the models. This shows us that while both models can give good approxi-

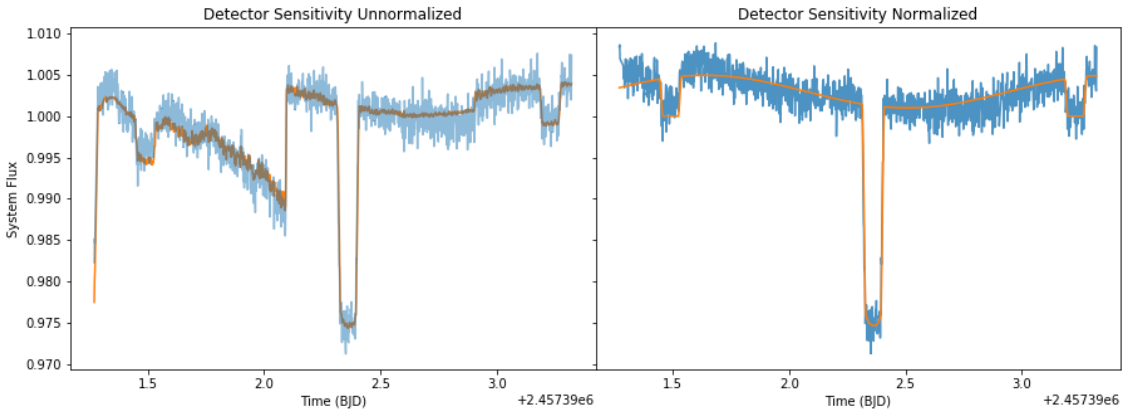

(a) Quadratic polynomial model.

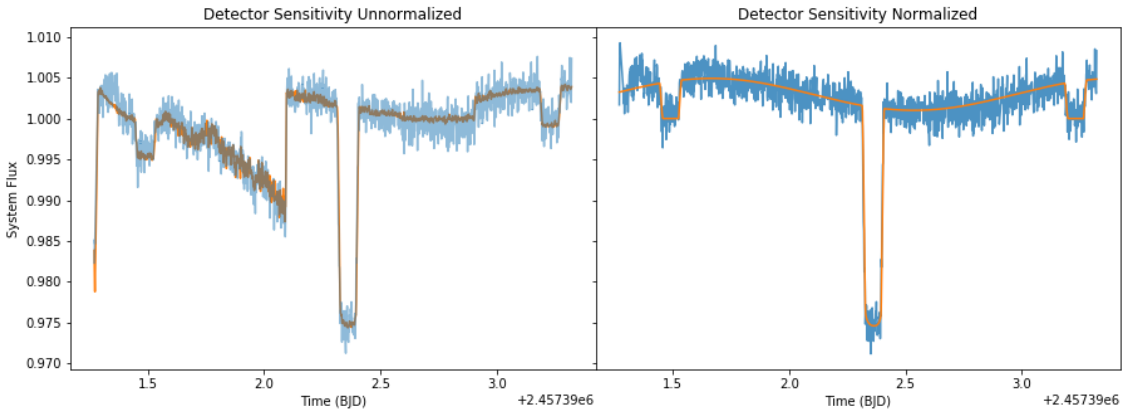

(b) Cubic polynomial model.

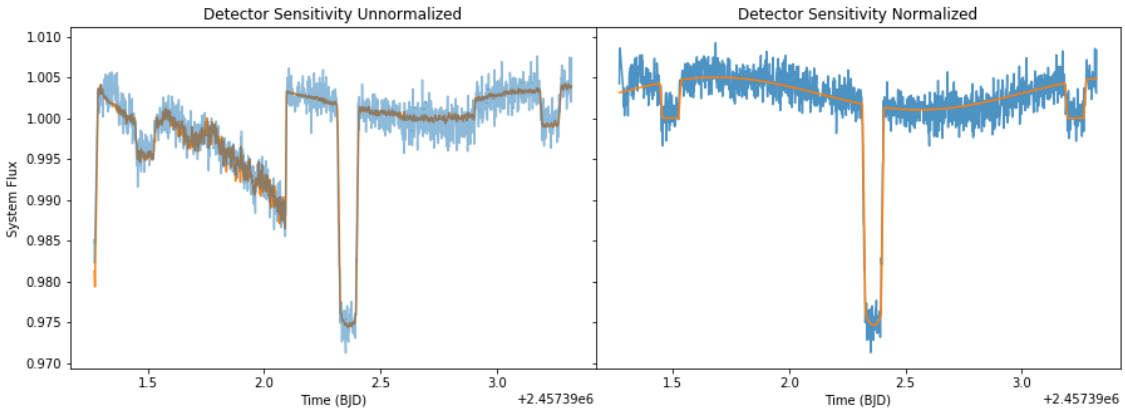

(c) Quartic polynomial model.

FIG. 3: CoRoT-2b transit lightcurves fitted with polynomial-type sensitivity models. The blue curves are the raw transit lightcurves with white noise added and the orange curves are the MCMC fits. The left plots show data with the sensitivity model included whereas the right plots divide out the sensitivity model to show the true astrophysical signal.

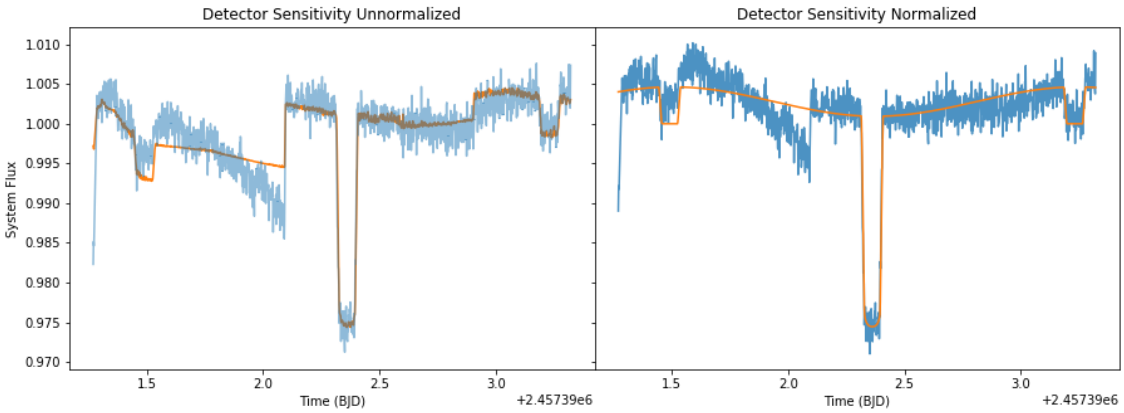

(d) Fourier n=2 model.

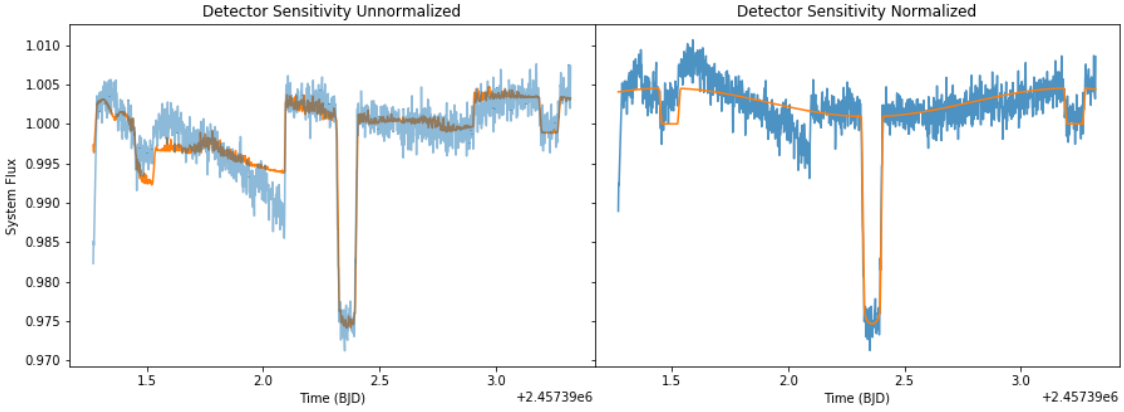

(e) Fourier n=3 model.

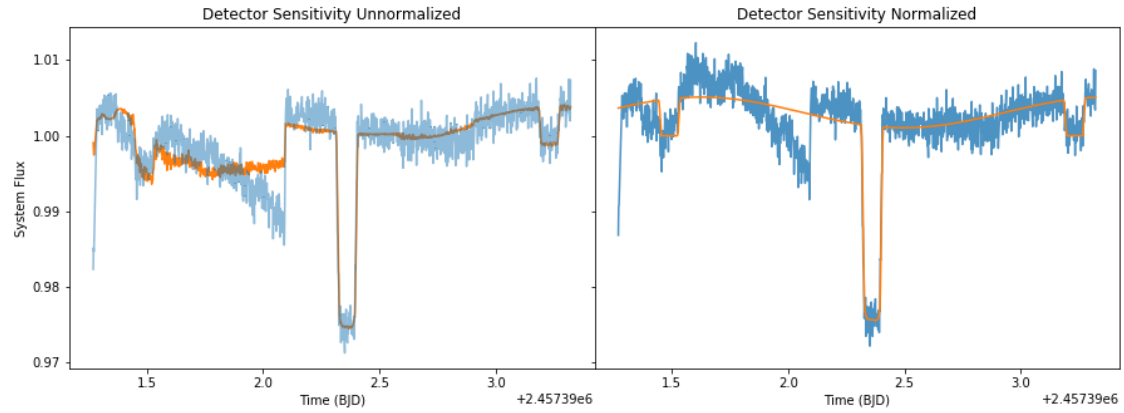

(f) Fourier cosine model.

FIG. 3: CoRoT-2b transit lightcurves fitted with Fourier-type sensitivity models. The blue curves are the raw transit lightcurves with white noise added and the orange curves are the MCMC fits. The left plots show data with the sensitivity model included whereas the right plots divide out the sensitivity model to show the true astrophysical signal.

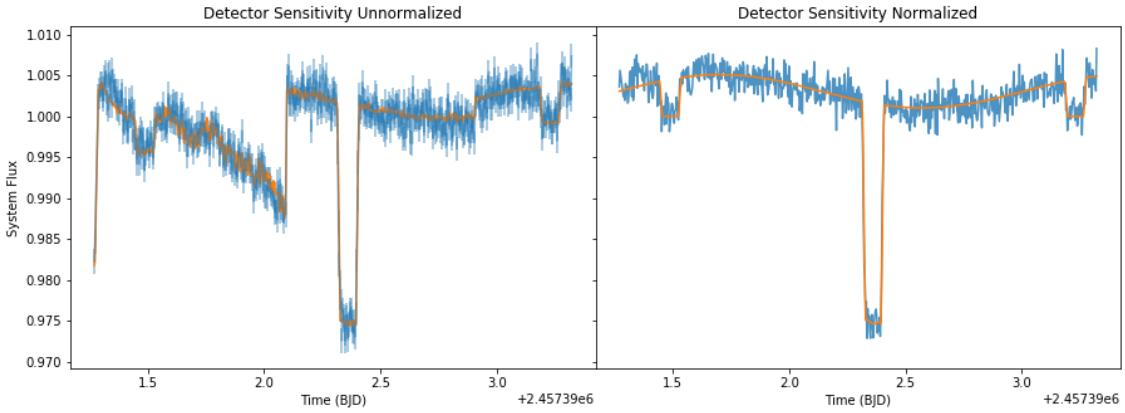

(g) Gaussian Process model.

FIG. 3: CoRoT-2b transit lightcurves fitted with the Gaussian Process sensitivity model. The blue curves are the raw transit lightcurves with white noise added and the orange curves are the MCMC fits. The left plots show data with the sensitivity model included whereas the right plots divide out the sensitivity model to show the true astrophysical signal.

mations to the raw transit data, it could be misleading to blindly accept results without trying other detector sensitivity models. There is merit to testing how different methods of handling data affect one's interpretation of the data.

In an ideal world with access to infinite computing power, researchers would not have to worry about trying too few variations of their simulations. However, we do not live in an ideal world, and the discussion of runtime is important. For the detector sensitivity models we have laid out so far, the quadratic model was by far the fastest to run. This is easily due to the simplicity of the model; quadratic being the lowest degree polynomial model and polynomials being less computationally expensive than sines or cosines. However, the GP model overshadowed all other models for being the most computationally expensive, taking over three hours to run 1000 MCMC steps and over five hours to run 1500 MCMC steps, both with 50 walkers. In comparison, the polynomial and Fourier models each took, at maximum, 30 minutes to run 6000 steps with 70 walkers. Because of this, we resorted to using only half the raw data for the MCMC by compiling every second data point.

Deciding on which model is superior is murky. On one hand, the GP model seems to most accurately fit the transit data qualitatively. Moreover, its fit parameters are consistent with most of the other models used in this project. However, the runtime for the GP model only became manageable once we reduced the amount of data used. This was on top of the fact that the CoRoT-2b dataset was the smallest out of the three exoplanet datasets. If time is not a limiting factor, then the lack of structure the GP model provides would be a solid sensitivity model to use for future exoplanet analyses. Unfortunately, time is usually a limiting factor for most cases. If one is not content with lowering the data resolution just to use the GP model (maybe the results are super sensitive to data), one may have to resort to using the polynomial or the Fourier models.

Between the polynomial and Fourier models, the polynomial models fit the data more cleanly. But this is not to say that the Fourier models do not fit the data; the fits for the true astrophysical signal (the orange curves) are pretty indistinguishable from the polynomial model fits. Also, the fact that the Fourier models were more discriminatory to white noise is a potential advantage that cannot be overlooked. In conjunction with the fact that the Fourier cosine model is consistent with the quadratic polynomial model when it comes to the fit parameters, it seems unwise to purely favour one over the other. With more refining, the Fourier models could begin to fit the data just as well as the polynomial models. For now, however, we recommend using the polynomial sensitivity models due to their faster runtimes and greater fit consistencies.

The main take away from model comparison is that one should always test a wide variety of different analysis methods before committing to a result. Future extensions to this project would be to improve the Fourier models and invent new ones. One way the Fourier models could be improved is to have more than two or three terms in the series. Theoretically, the full Fourier series require an infinite amount of terms for exact convergence. In practice, ten to twenty terms should suffice for a good approximation, depending on the data, but having just two terms is not sufficient. Most of the drawbacks mentioned for the Fourier models may just be the result of not having enough terms to work with.

B. Exoplanetary Winds

To compare the strength of exoplanetary winds between each exoplanet, we must decide on a detector sensitivity model we believe to be the most reliable. We chose the polynomial model (specifically the quadratic model) to be our standard due to it being the fastest to run and fitting the raw data reasonably well. The quadratic model fits for CoRoT-2b, KELT-9b, and WASP-18b are shown in Fig. 4.

In Fig 5, offsets are plotted against dayside-nightside temperature differences for all three polynomial sensitivity models. A trend can be seen where larger temperature differences correlate with smaller offsets. This seems counter-intuitive because larger temperature differences lead to stronger winds due to steeper temperature gradients, which in turn should offset the transit curves more. However, the data is seemingly telling us that stronger winds cause smaller offsets (true for all three planets). This may be because stronger winds transfer more heat from the dayside to the nightside, leaving the planet with less drastic temperature differences.

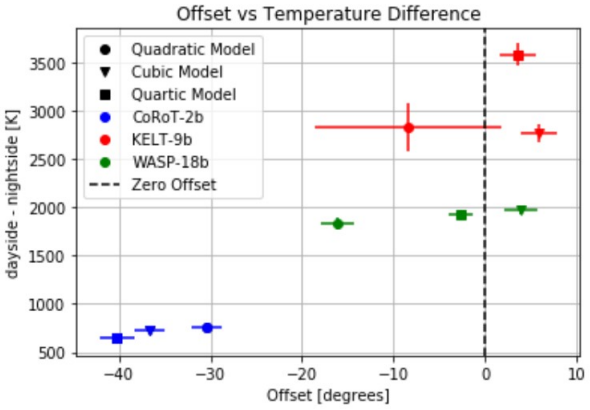

FIG. 5: Plot showing the peak lightcurve offset from the phase of eclipse vs. the difference in dayside and nightside temperatures. CoRoT-2b is graphed in blue, KELT-9b in red, and WASP-18b in green. Although the main results are from the quadratic sensitivity model, the rest of the polynomial models are shown for reference. Some vertical error bars are too small to be seen.

The sign of the offset tells us information about the wind's direction. As a reminder, a positive offset means that the lightcurve peaks before the secondary transit dip (eclipse) and a negative offset means that the lightcurve peaks after the eclipse. This is true because we are working with tidally-locked planets and the peak of the secondary lightcurve is where the observer would receive the maximum flux from the planet's surface. Seeing as how all three planets have negative offsets for the quadratic model, the wind is mostly likely to be blowing westward for all three planets.

While all of these are valid conclusions, nothing concrete can be said until we acquire a larger sample of exoplanets because we are doing population statistics with only three samples. Moreover, there are many other factors in play such as wind travelling in both directions, like in Jupiter, as well as the composition of the atmosphere affecting the planet's ability to retain heat.

IV. CONCLUSION

In this paper, we examined how different detector sensitivity models affected the analysis of CoRoT-2b transit data, as well as comparing the planetary wind properties of three exoplanets. We came to the conclusion that the Gaussian Process model was the model of choice if runtime was not an issue. We also found that using different sensitivity models could result in significantly different determinations of the fit parameters, even when both models appeared to fit the data well. This showed the importance of trying out other sensitivity models for transit data analysis to ensure that a determined parameter is not an outlier.

Analysis of the dayside and nightside temperatures and offsets across the different planets showed an unexpected trend of lower offsets appearing to have greater temperature differences. This is counter-intuitive to the idea that larger temperature differences cause stronger winds, therefore making the peak flux further away from the eclipse. Moreover, the negative offsets seem to imply westward-blowing wind for all three exoplanets. However, given the fact that only three exoplanet data was used and the offset values were sensitivity model dependent, it is unreasonable to make any real conclusions until more planets are compared.

Author Contribution Statement

All authors worked on the original Coding Lab separately and then compared ideas for the final copy. Lambert made the code more modular to facilitate procedure automation. Kevin created the Fourier sensitivity models and worked on implementing the Gaussian Process model. Emma worked on the exoplanetary winds section. Many laptops suffered for this project. All authors contributed to the paper, with Kevin and Emma mainly working on the Introduction and Lambert mainly working on the Methods and Conclusion. For the Results & Discussion, Kevin and Lambert focused on Model Selection and Emma focused on Exoplanetary Winds. Kevin spent way too many hours editing the paper. Special credits go to Taylor for debugging our code when we got stuck and answering all our questions.

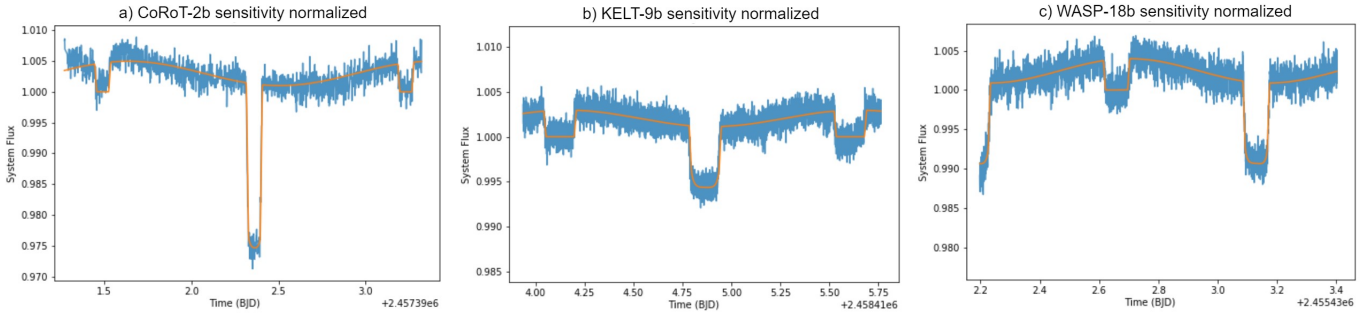

FIG. 4: Quadratic model fits for all three exoplanets. Note that the vertical axis scale is different for each plot. CoRoT-2b is seen to have a much deeper primary transit than the other two, and WASP-18b has the most shallow primary and secondary transits. a) $\sigma = 1.29(3) \times 10^{-6}$ b) $\sigma = 4.5(1) \times 10^{-7}$ c) $\sigma = 7.8(2) \times 10^{-7}$

[1] What is the Transit Method? - Universe Today.

[2] M. Ramadevi, Limb darkening, (2018).

[3] M. Richmond, Limb darkening, Available at `http://spiff.rit.edu/classes/phys440/lectures/limb/limb.html` (2020-04-08) (2014).

[4] R. Alonso, Characterization of exoplanets: Secondary eclipses, in *Handbook of Exoplanets*, edited by H. J. Deeg and J. A. Belmonte (Springer International Publishing, Cham, 2018) pp. 1–26.

[5] A. K. Singal, Life on a tidally-locked planet, arXiv e-prints , arXiv:1405.1025 (2014), arXiv:1405.1025 [physics.pop-ph].

[6] B. M. Kilpatrick, N. K. Lewis, T. Kataria, D. L. Deming, J. G. Ingalls, J. E. Krick, and G. S. Tucker, Spitzer secondary eclipse depths with multiple intrapixel sensitivity correction methods: Observations of wasp-13b, wasp-15b, wasp-16b, wasp-62b, and hat-p-22b (2016).